Cosmic-ray Ionization Rates with H_3^+: an Expanded Sample

Nick Indriolo*, Paola Caselli, Alexei Ivlev, Arshia Jacob, David Neufeld, Marta Obolentseva, Kedron Silsbee, & Mark Wolfire

*Space Telescope Science Institute

Outline

- Motivation & Background
- Observations
- Analysis & Results
- Summary & Future Prospects

Motivation

- The ionization of atomic and molecular gas in the ISM by cosmic rays influences various physical and chemical processes, e.g.,
  - increases chemical complexity
  - affects coupling between gas and magnetic fields
- Cosmic rays provide a source of pressure that may be able to drive large scale galactic outflows. This can act as a potential feedback mechanism to quench star formation

Particle Interactions

- Ionization

  $p + H_2 \rightarrow H_2^+ + e^- + p'$

- Spallation and Fusion

  $[p, \alpha] + [^{12}C, ^{14}N, ^{16}O] \rightarrow [^{6}Li, ^{7}Li, ^{9}Be, ^{10}B, ^{11}B]$

- Nuclear Excitation

  $[p, \alpha] + {}^{12}C \rightarrow {}^{12}C^* \rightarrow {}^{12}C + \gamma_{4.44\ \mathrm{MeV}}$

- Inelastic Collisions

  $p + H \rightarrow p' + H + \pi^0$

  $\pi^0 \rightarrow \gamma + \gamma$

More Particle Interactions

- Inverse Compton scattering

$$e^- + \gamma_{Elo} \rightarrow e^- + \gamma_{Ehi}$$

- Synchrotron radiation
- Bremsstrahlung
- Inner-shell ionization (e.g., Fe Kα)

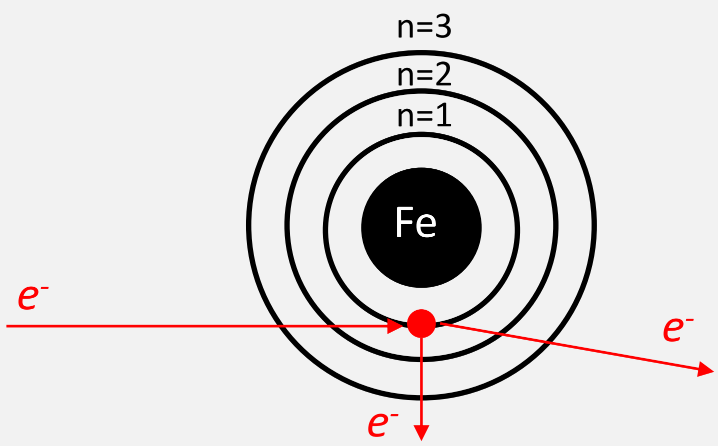

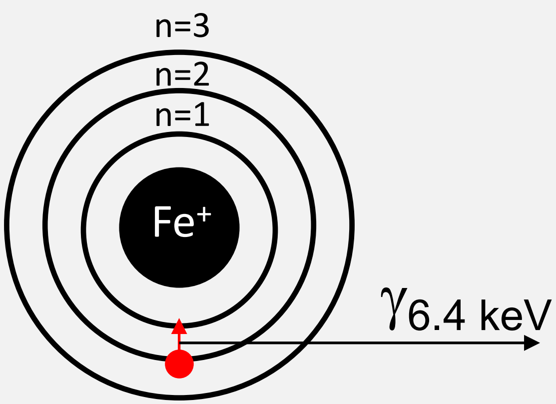

Observables

- Gamma-ray emission from molecular clouds
  - Result of π_0 production and decay
  - Active when CR proton has $E > 280$ MeV
- Emission/absorption lines from molecules with abundances controlled by CR ionization of H and H_2
  - Result of ion-molecule chemistry
  - Dominated by protons with $1 < E < 100$ MeV
- Different observables trace different portions of the cosmic-ray spectrum

Hydrogen Chemistry

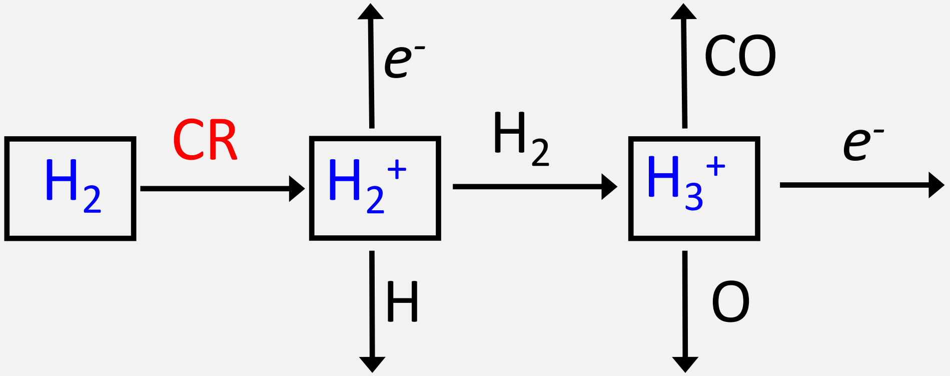

- Formation
  - $CR + H_2 \rightarrow H_2^+ + e^- + CR'$
  - $H_2^+ + H_2 \rightarrow H_3^+ + H$
- Destruction
  - $H_3^+ + e^- \rightarrow H + H + H$

- Dense Clouds
  - $H_3^+ + CO \rightarrow HCO^+ + H_2$
  - $H_3^+ + O \rightarrow OH^+ + H_2$
- Atomic Clouds
  - $H_2^+ + H \rightarrow H_2 + H^+$
  - $H_2^+ + e^- \rightarrow H + H$

Analytical Approximation to ζ

- Approximation in diffuse molecular clouds assumes steady-state chemistry, 100% efficiency factor in forming H_3^+, and destruction by electron recombination

$$\zeta(\mathrm{H_2})n(\mathrm{H_2}) = k(\mathrm{H_3^+}|e^-)n_e n(\mathrm{H_3^+})$$

- Recast in terms of column densities and electron fraction with respect to total hydrogen density

$$\zeta(\mathrm{H_2}) = k(\mathrm{H_3^+}|e^-)x_e n_H \frac{N(\mathrm{H_3^+})}{N(\mathrm{H_2})}$$

- Superseded by more detailed chemical models (see Wed. talks by Arshia Jacob and Alexei Ivlev), but sufficient for a preliminary analysis

Analytical Approximation to ζ

$$\zeta(\mathrm{H_2}) = k(\mathrm{H_3^+}|e^-)x_e n_H \frac{N(\mathrm{H_3^+})}{N(\mathrm{H_2})}$$

- $k(\mathrm{H_3^+}|e^-)$ has been measured in laboratory experiments
- x_e is inferred from average $\mathrm{C^+}$ abundances
- n_H can be inferred from the relative populations in different rotational states of molecules, e.g., $\mathrm{C_2}$ (Neufeld et al. 2024 ApJ 973, 143)
- $N(\mathrm{H_2})$ measured from UV absorption line observations
- $N(\mathrm{H_3^+})$ measured from IR absorption line observations

Observing H_3^+

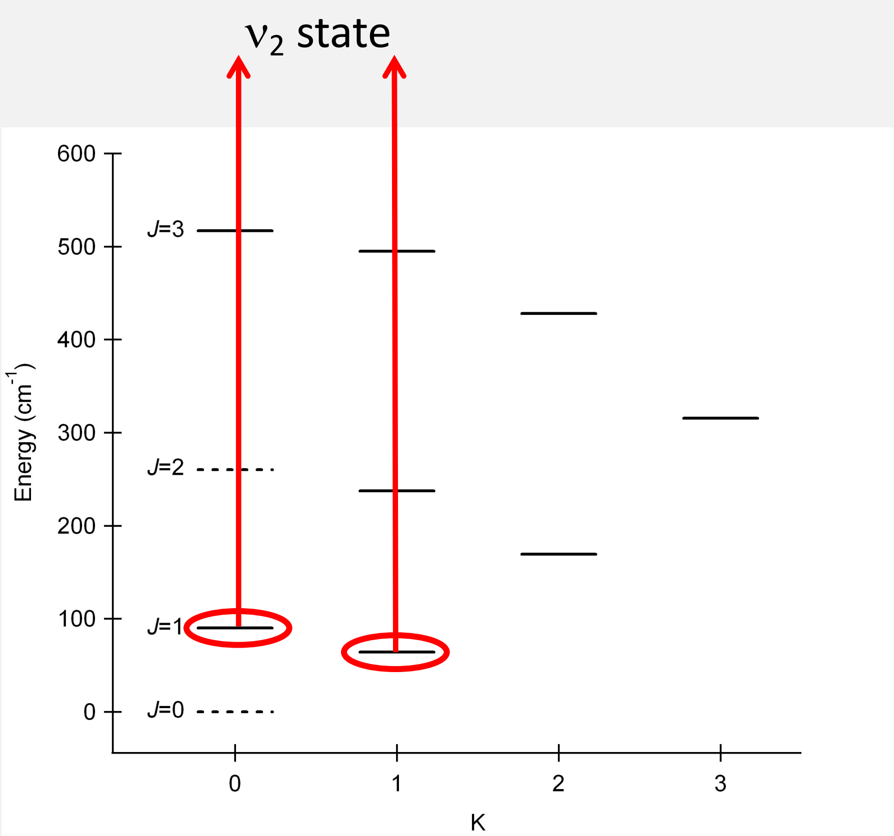

Energy level diagram for the ground vibrational state of H_3^+

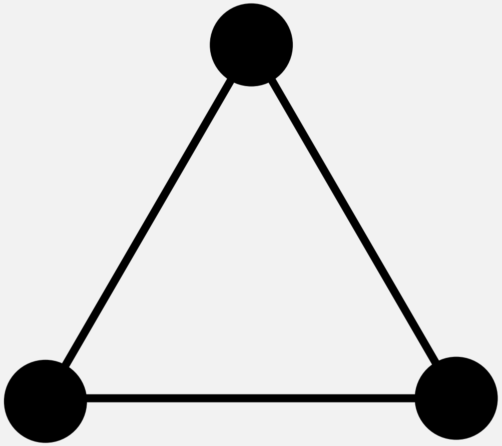

- No permanent dipole moment
- (*J*,*K*)=(0,0) state forbidden, requiring observations of both the (1,0) *ortho* and (1,1) *para* states to measure the total column density
- Target ro-vibrational transitions probing excitation to the ν_2 state

Observing H_3^+

- Transitions are in the 3.6-4.0 μm wavelength range
- Absorption lines are weak (1-2% deep at 4 km/s spectral resolution)
- Detecting H_3^+ absorption in the diffuse molecular ISM requires high S/N, high spectral resolution observations
- New H_2 results (Shull et al. 2021)
- IRTF/iSHELL

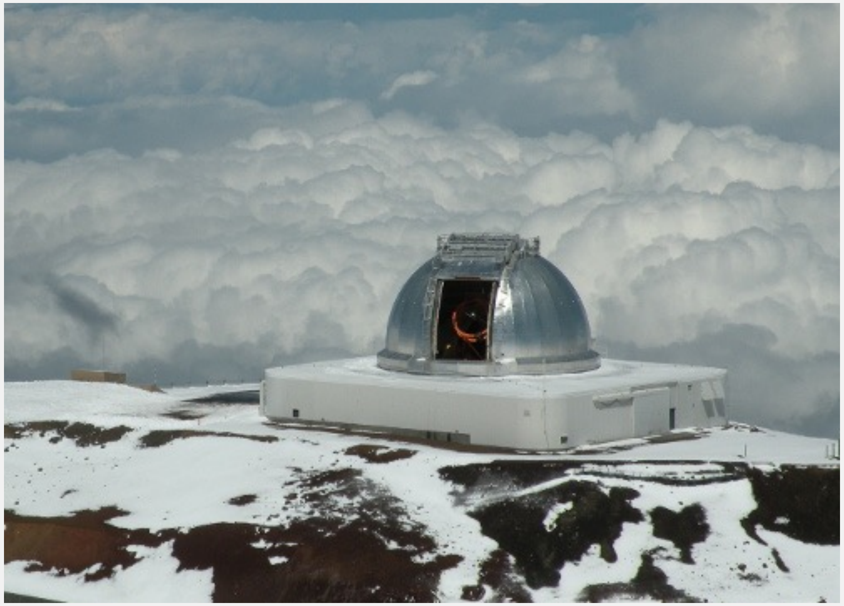

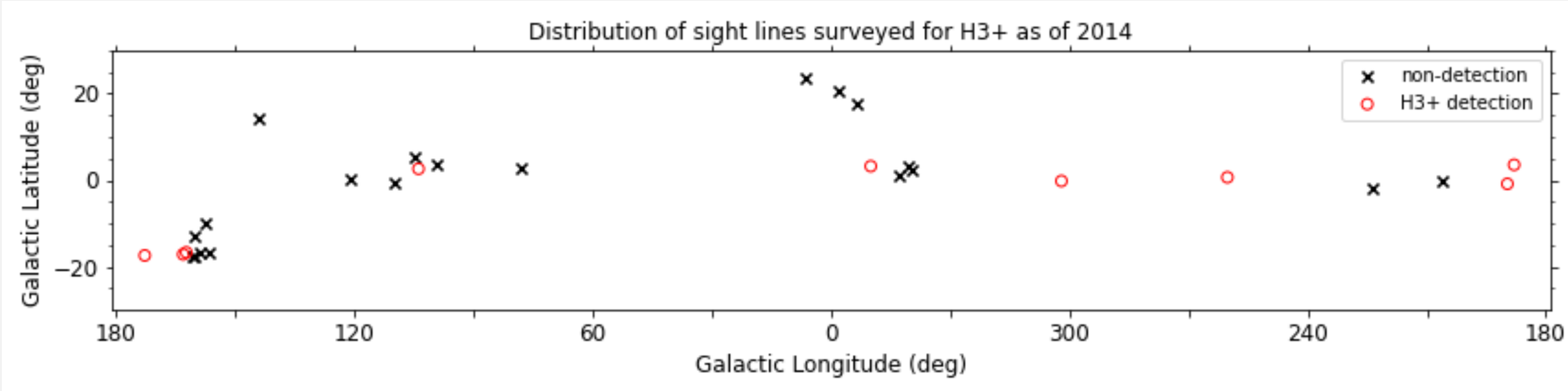

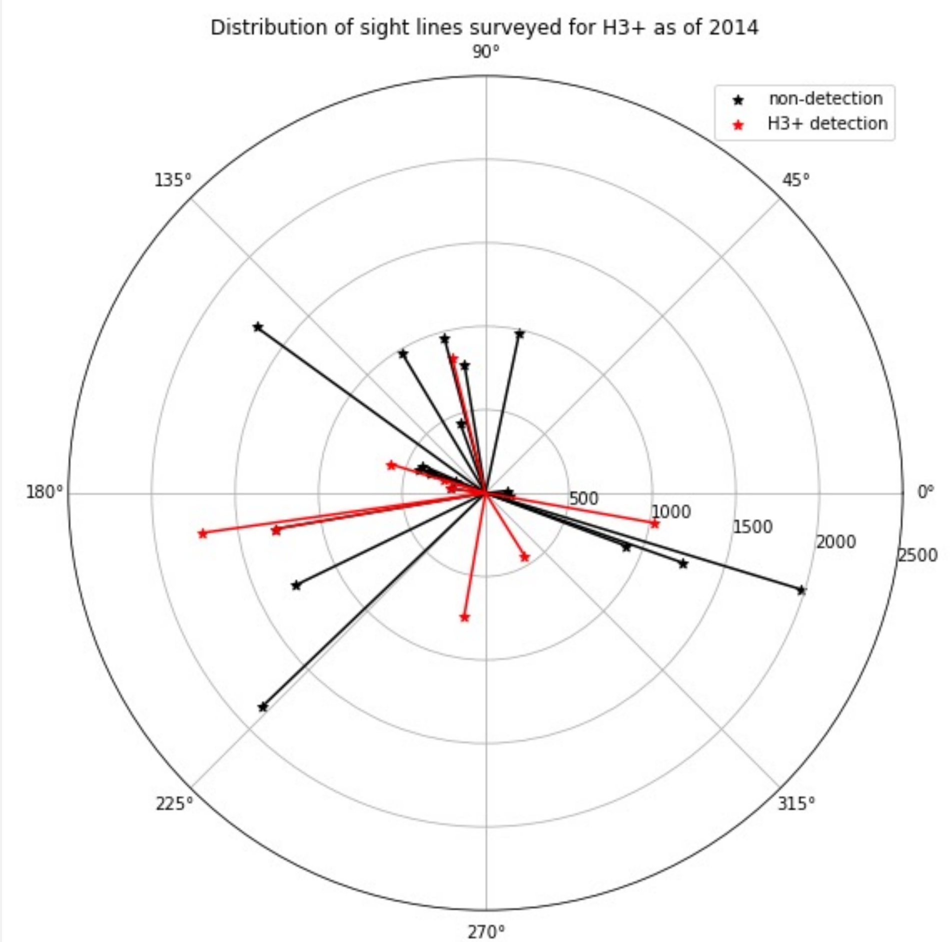

Sight lines with H_2 Observed

H_3^+ Detections: 9

H_3^+ Non-detections: 20

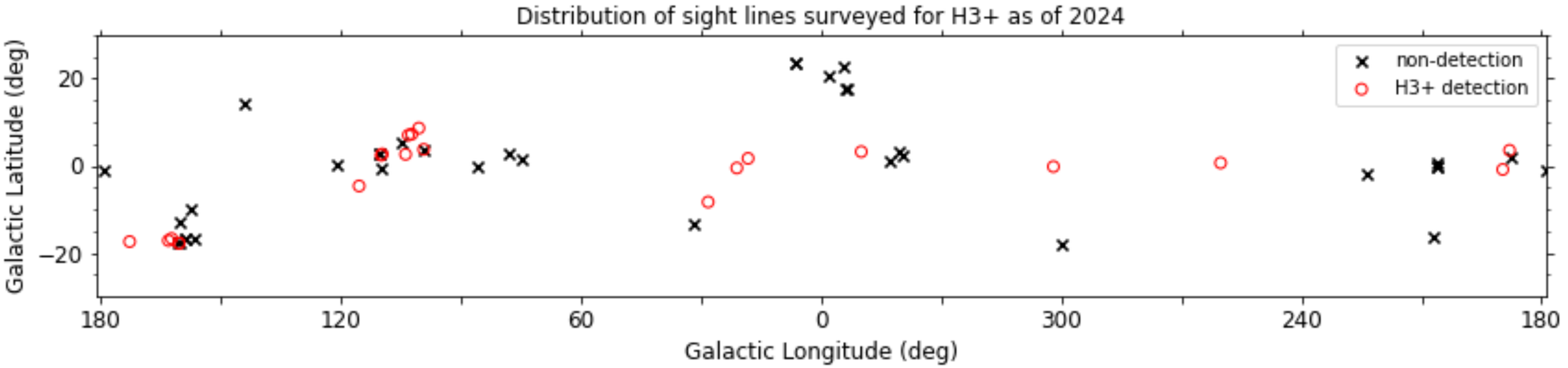

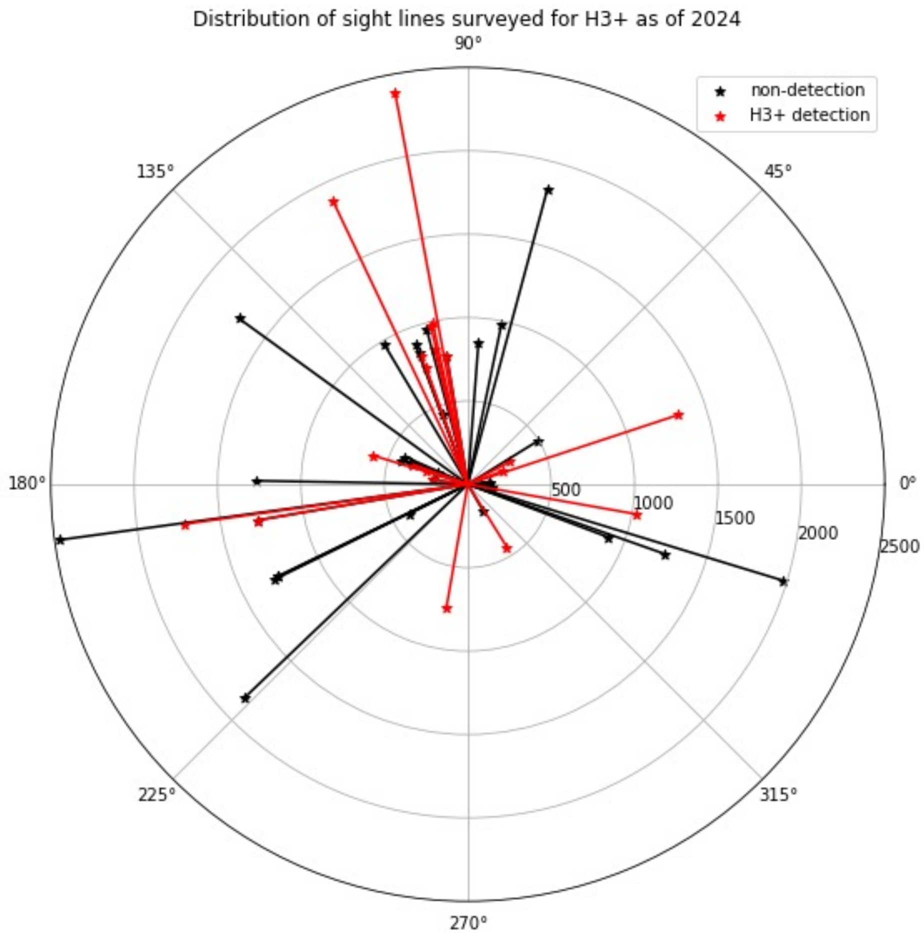

Sight lines with H_2 Observed

H_3^+ Detections: 21 (9+12)

H_3^+ Non-detections: 29 (20-3+12)

IRTF/iSHELL Observations

H_3^+ Detections

H_3^+ Non-detections

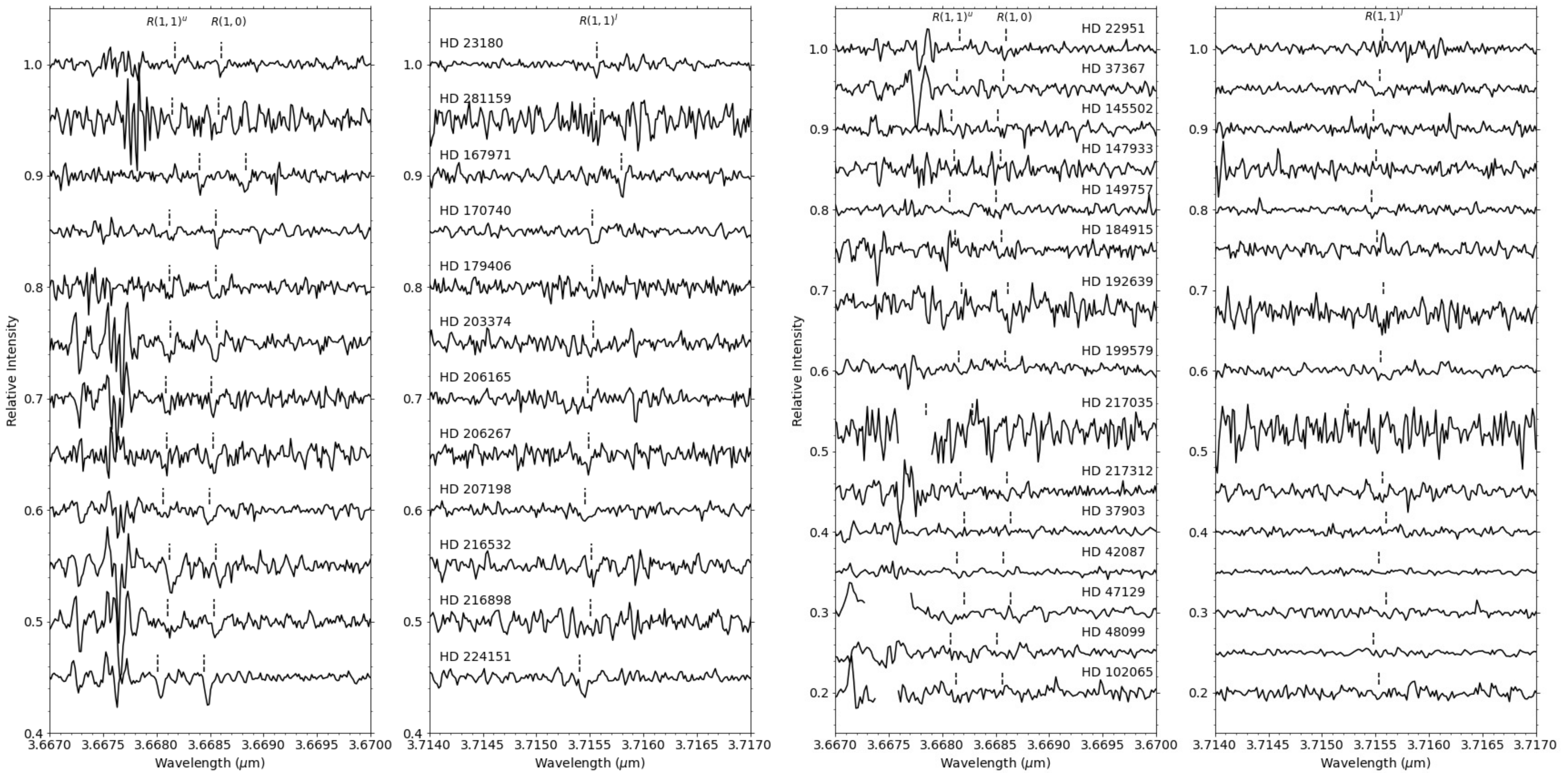

Indriolo et al. 2025 (in preparation)

$N(H_3^+)$ vs $N(H_2)$

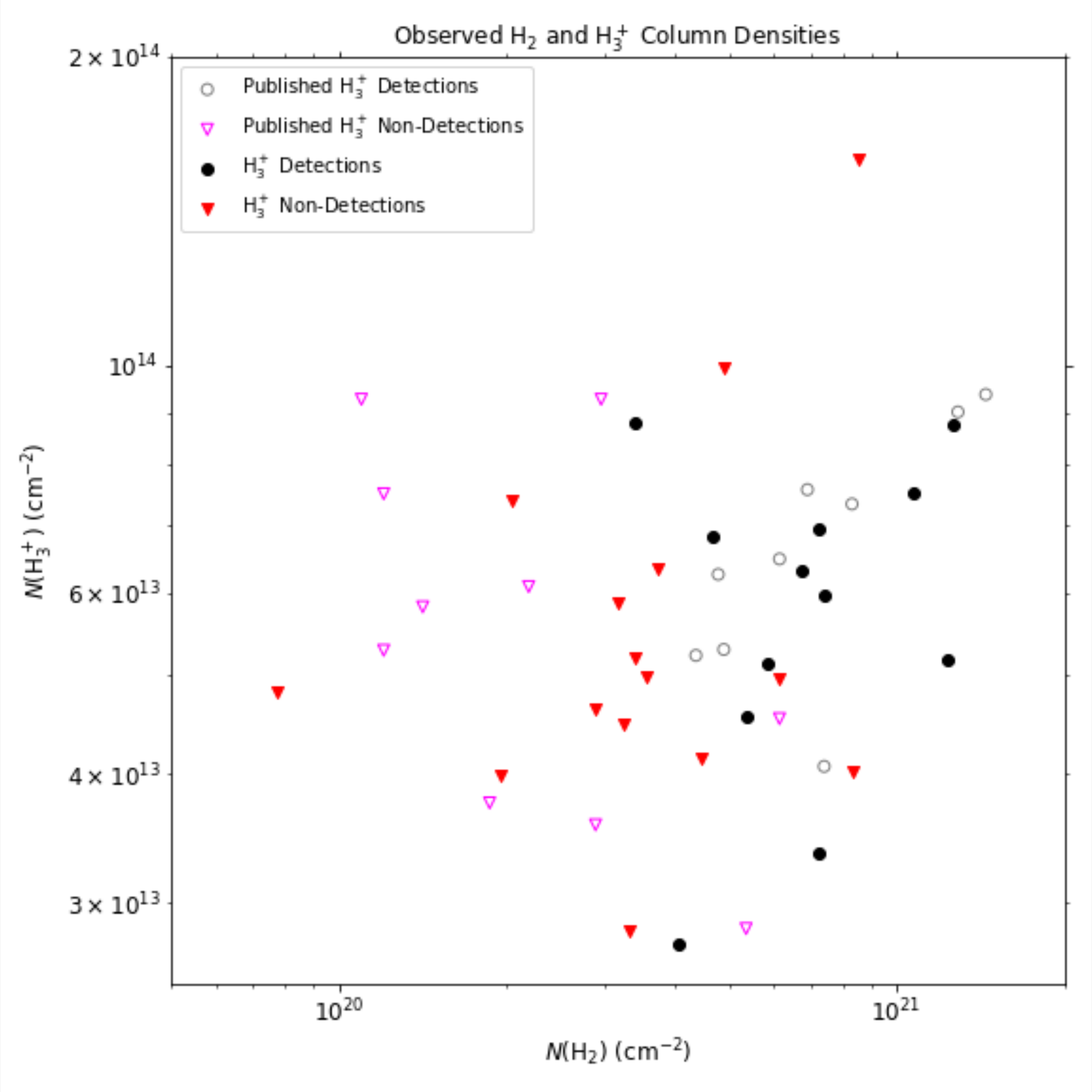

Observed H2 and H3+ Column Densities
Published H3+ Detections
Published H3+ Non-Detections
H3+ Detections
H3+ Non-Detections
2 × 10^14
10^14
6 × 10^13
4 × 10^13
3 × 10^13
N(H3+) (cm^-2)
10^20
10^21
N(H2) (cm^-2)

Pinpointing the Absorbing Gas

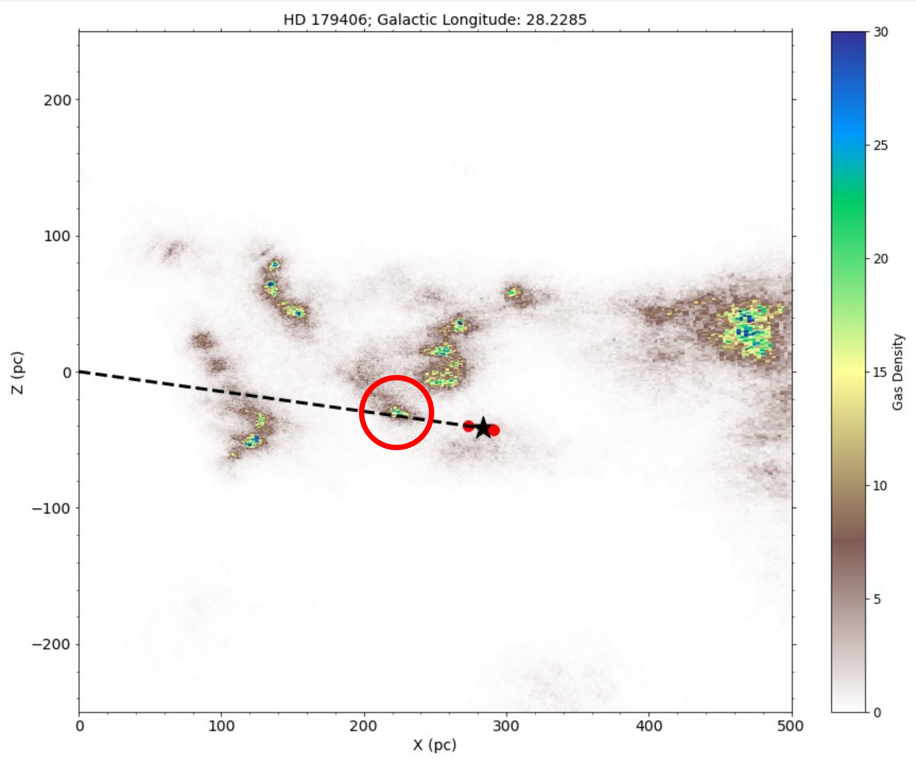

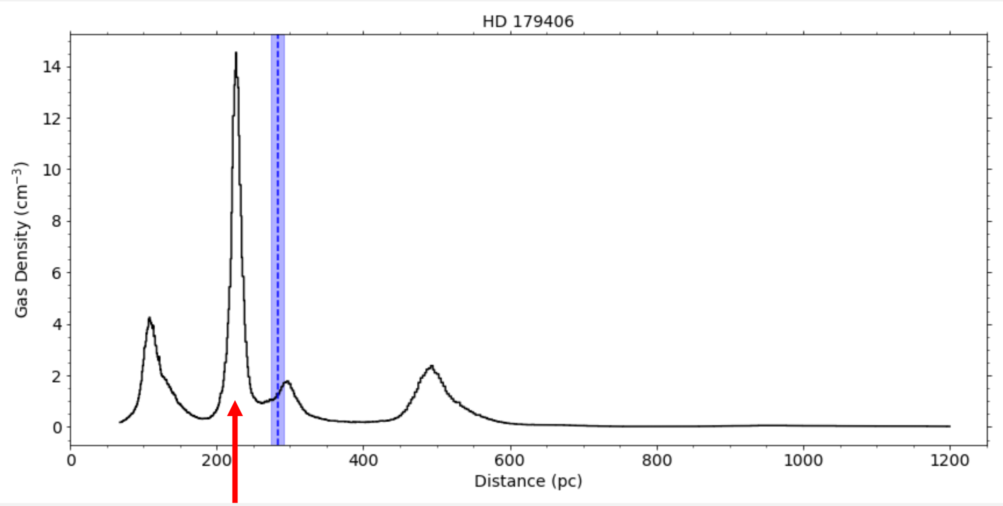

Densest gas is
at 226 pc

2D and 1D gas density profiles derived from Gaia extinction maps (Edenhofer et al. 2024)

See Alexei Ivlev's talk on Wednesday for what you can do with this information.

Complications

Cep OB3

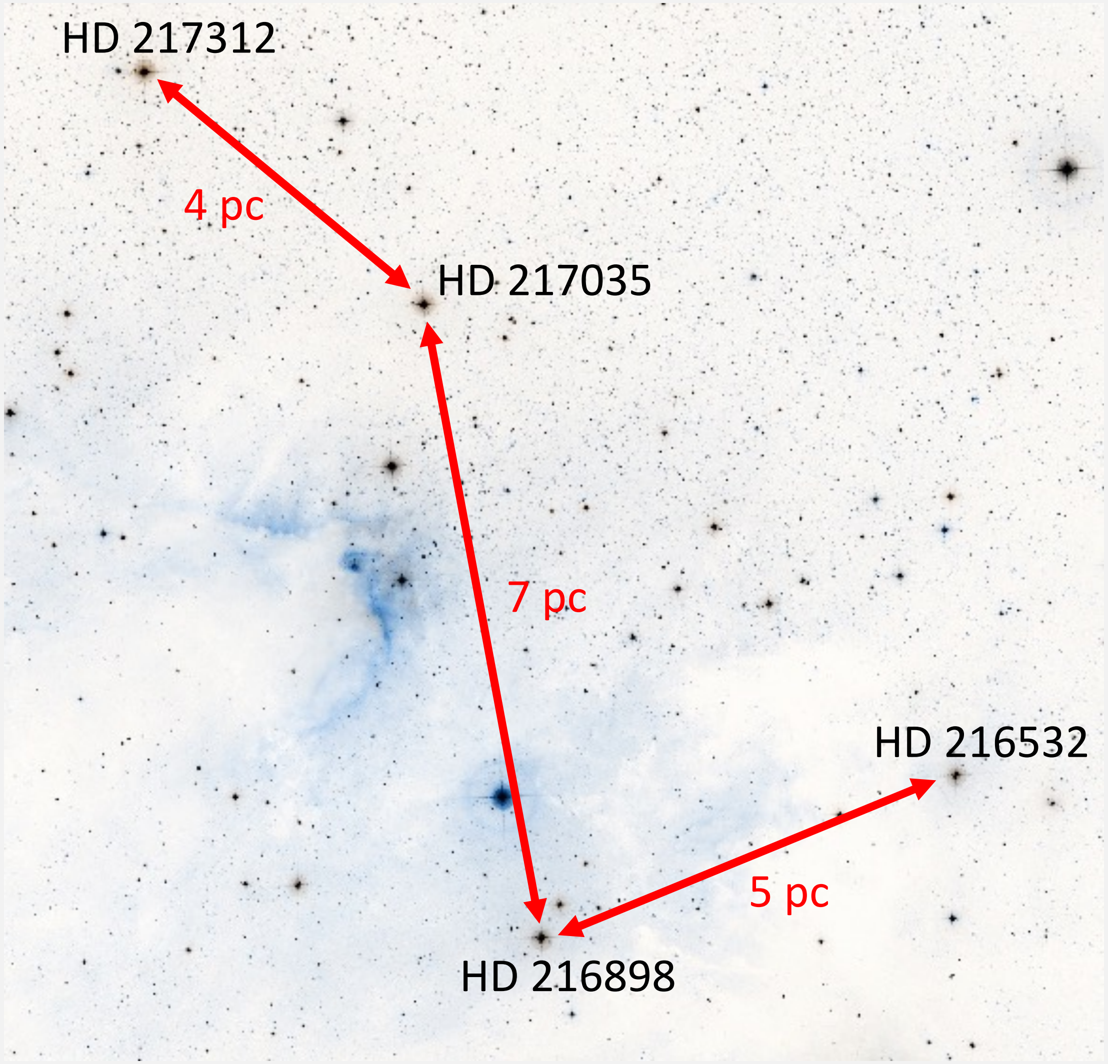

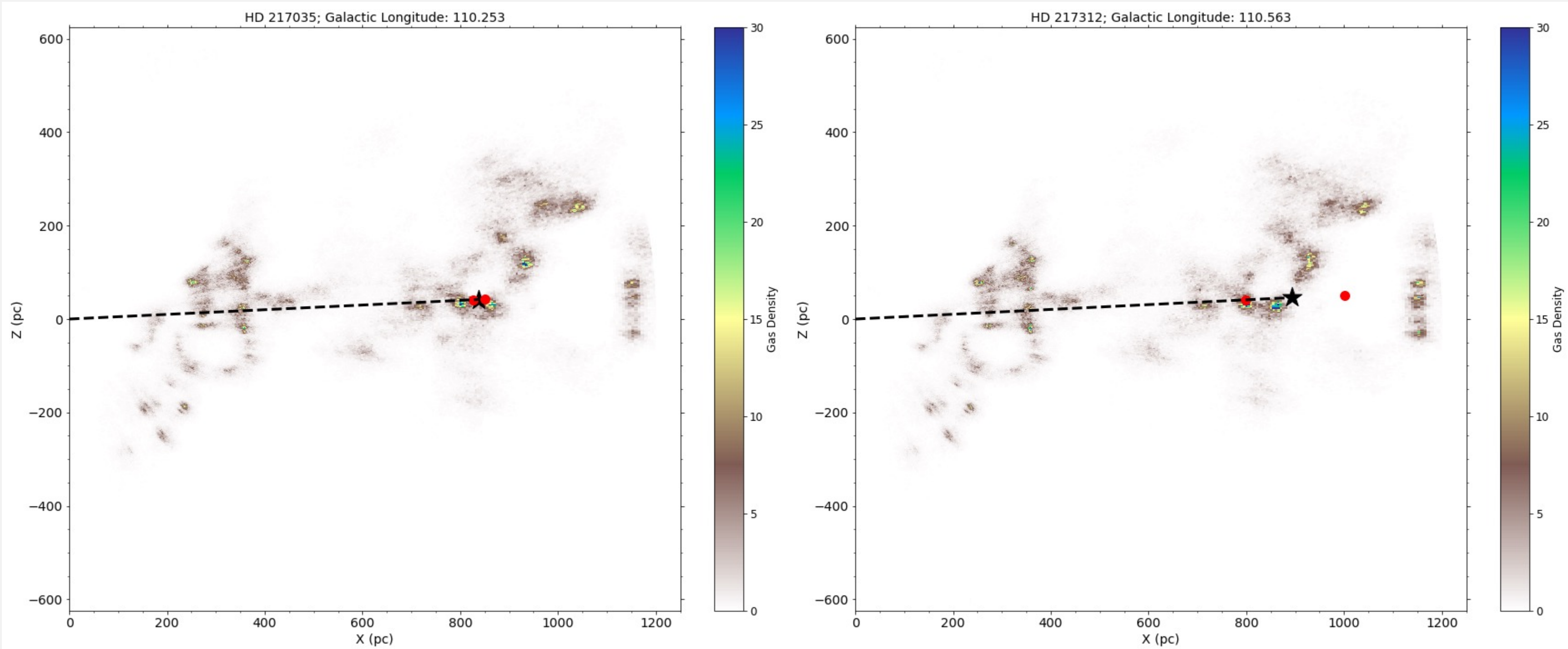
HD 217035; Galactic Longitude: 110.253
HD 217312; Galactic Longitude: 110.563
Z (pc)
X (pc)
Gas Density

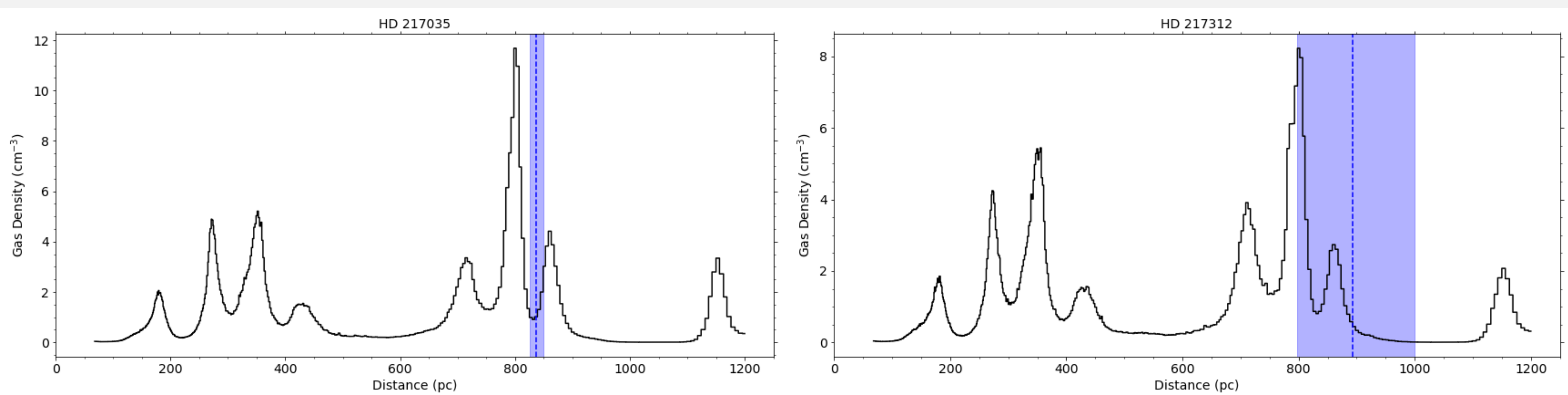
HD 217035
HD 217312
Gas Density (cm^{-3})
Distance (pc)

Complications

- In sight lines with multiple density peaks of similar magnitude and multiple absorption components it is non-trivial to associate the two
- How accurate are gas densities at farther distances in the Gaia extinction maps?

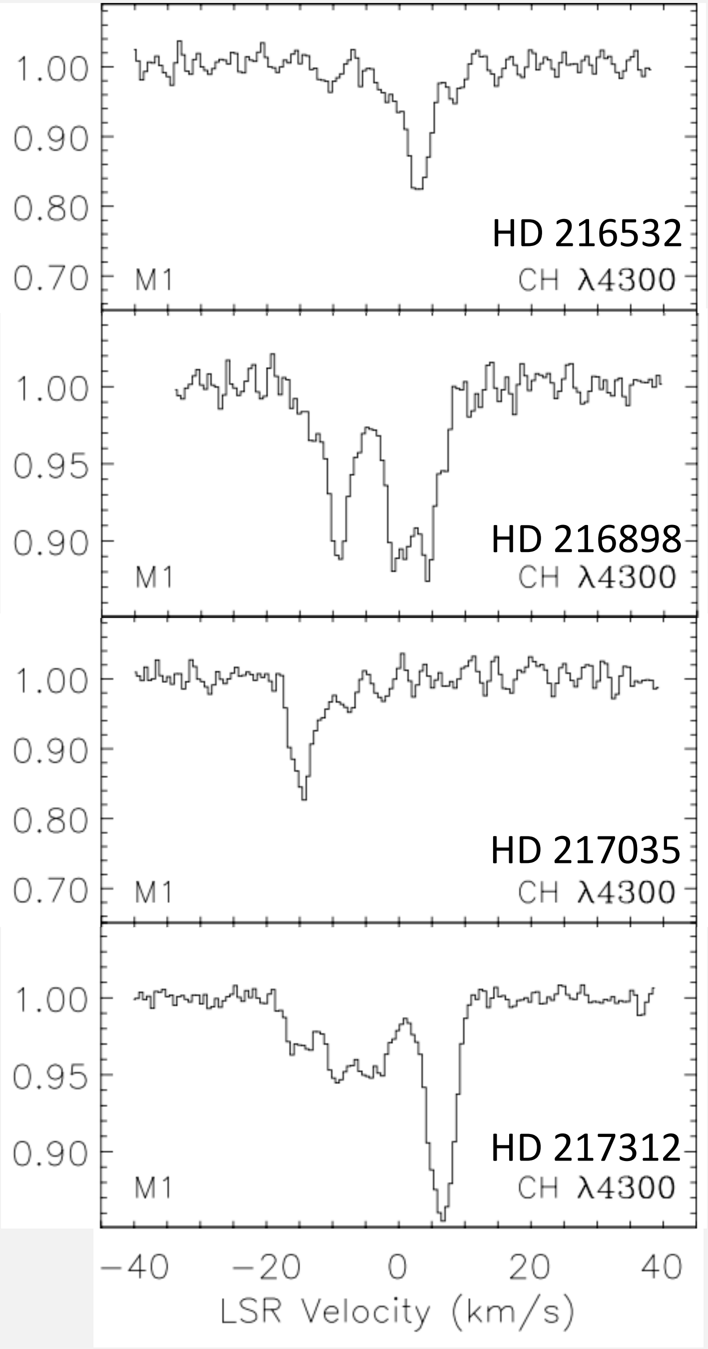

Pan et al. (2004)

Density Estimates

Neufeld et al. (2024)

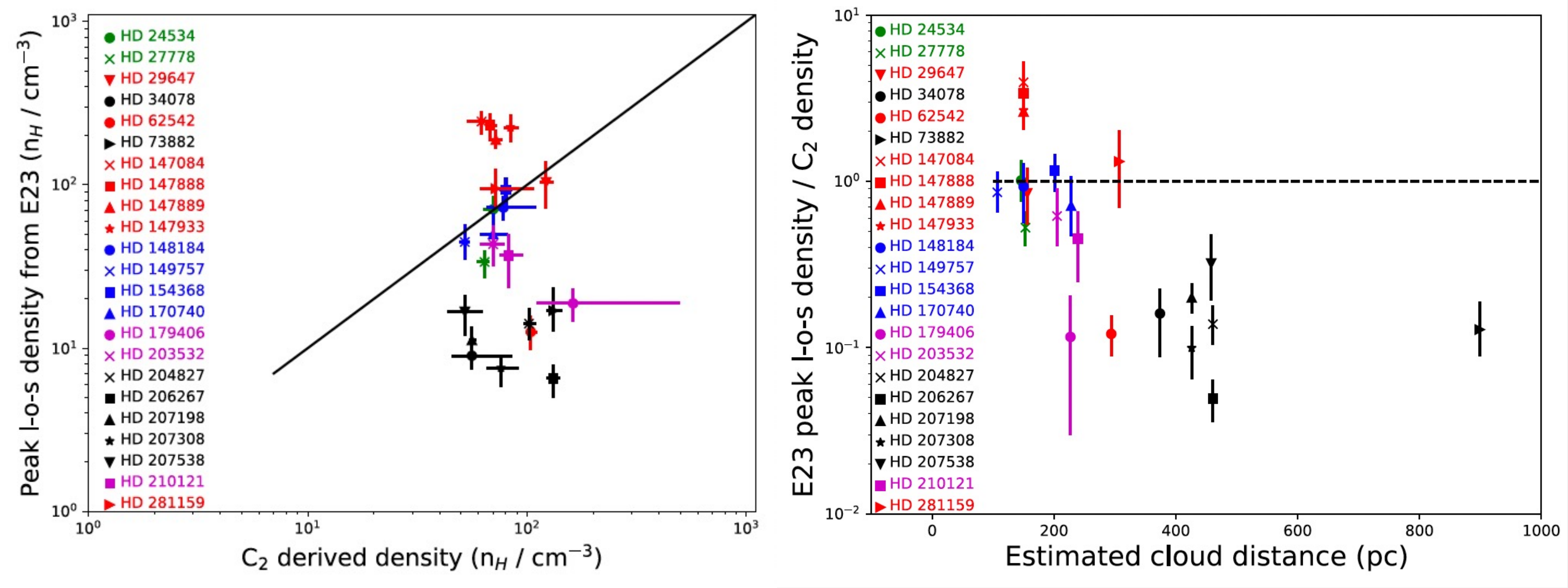

- Newly derived C_2 densities tend to be about 50-100 cm^{-3}, significantly below the average value of 200 cm^{-3} adopted by Indriolo & McCall (2012)
- Densities derived from C_2 excitation are not always consistent with those derived from extinction maps, which tend to be even lower
- Correlation between density ratio (Gaia / C_2) and distance to cloud suggests an effect from the resolution of the extinction map

Ionization Rates

$$\zeta(\mathrm{H_2}) = k(\mathrm{H_3^+}|e^-)x_e n_H \frac{N(\mathrm{H_3^+})}{N(\mathrm{H_2})}$$

- Inferred cosmic-ray ionization rates are directly proportional to the gas density
- Reduction in the inferred gas density leads to a corresponding reduction in the inferred cosmic-ray ionization rate
- Key finding of Neufeld et al. (2024) is that gas densities derived from C_2 using recently computed collisional rate coefficients drop by a factor of 4—7 compared to published results

Ionization Rates

	n_H	$\zeta(H_2)$
	(cm^{-3})	(10^{-17} s^{-1})
HD 23180	41	7.6
HD 281159	72	6.7
HD 167971	50	9.4
HD 170740	70	7.3
HD 179406	162	34.1
HD 206267	132	30.2
HD 207198	56	12.4
mean		**15.4**
Indriolo & McCall 2012		**35**
Obolentseva et al. 2024		**tomorrow**

Distribution of Ionization Rates

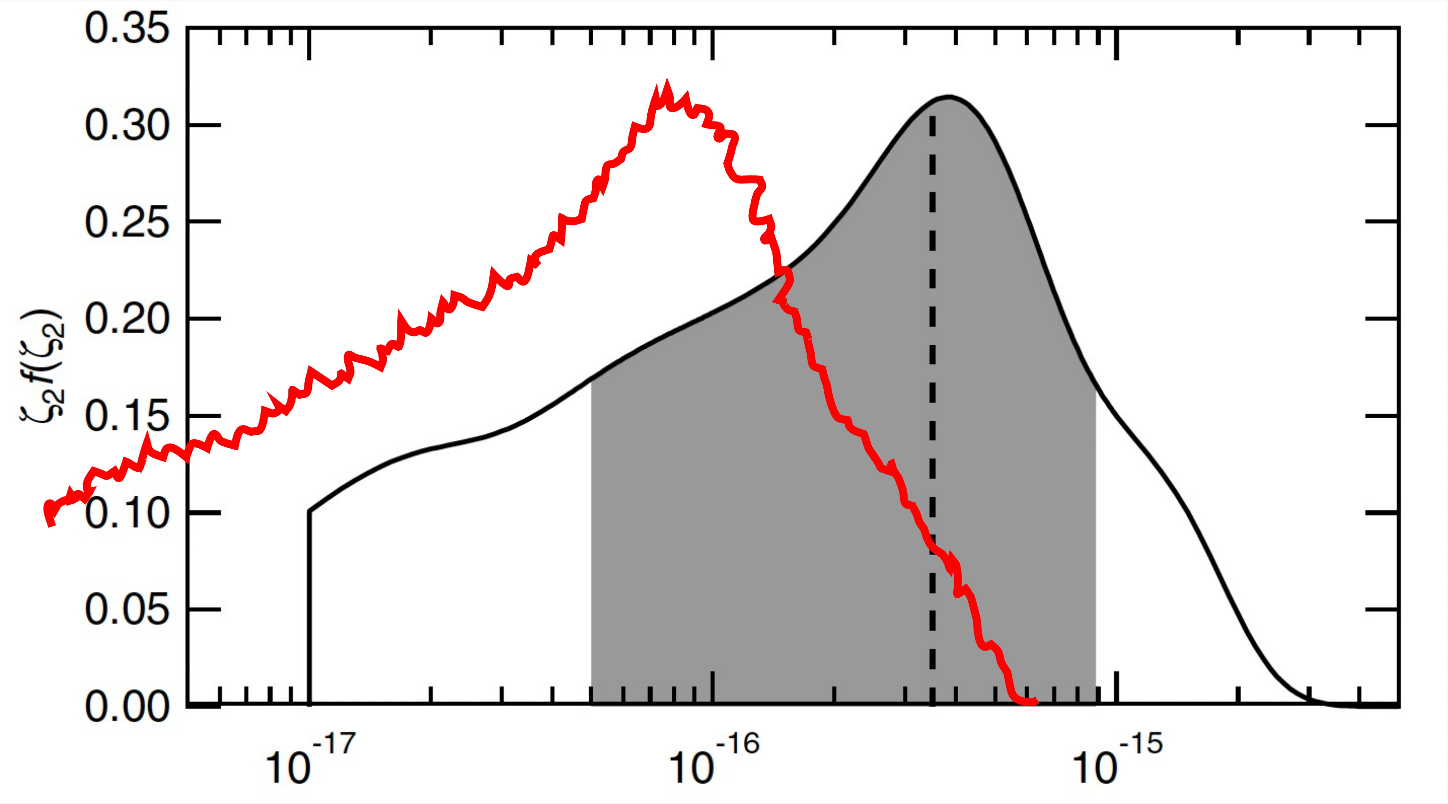

Indriolo & McCall (2012)

Map of Ionization Rates

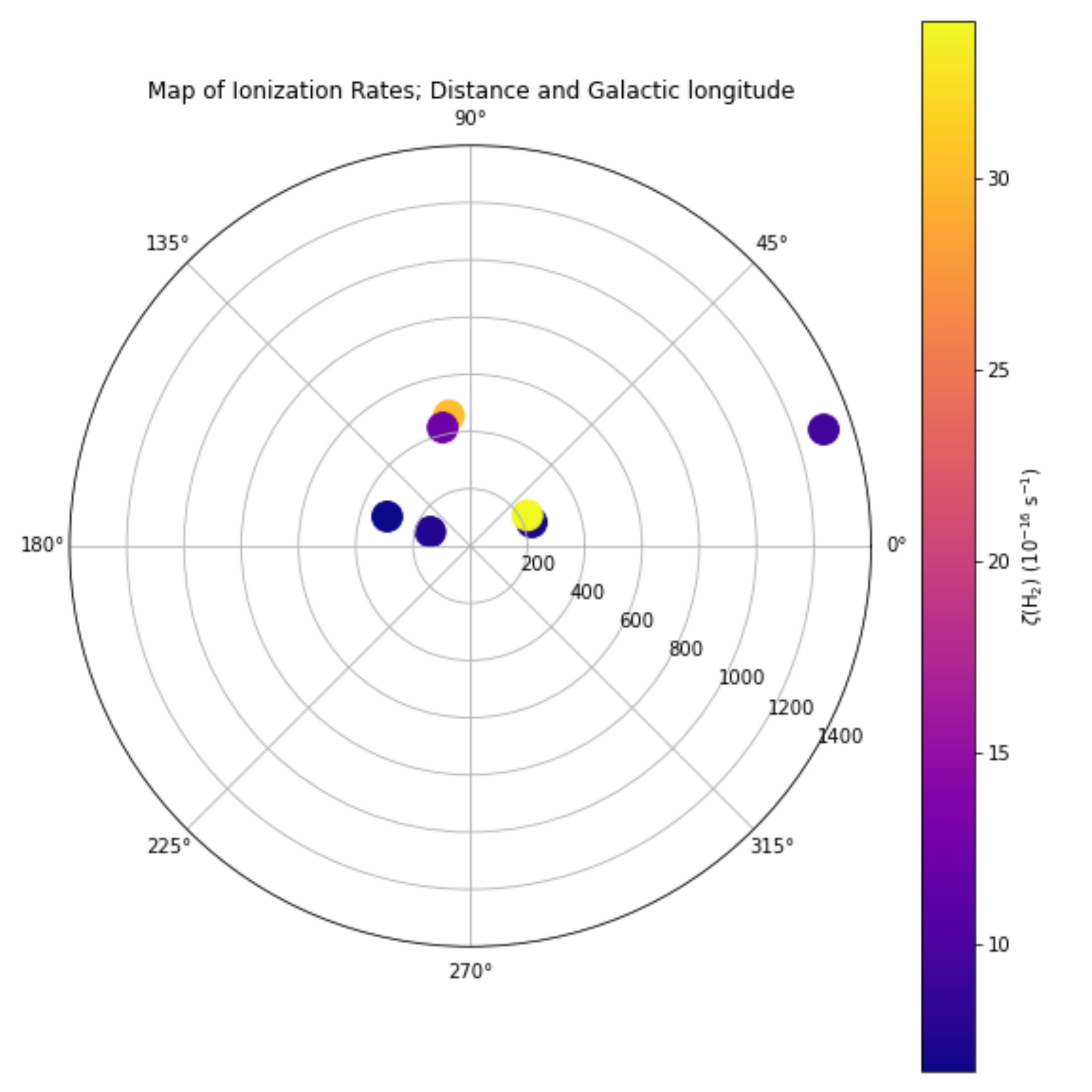

Summary

- New survey of diffuse cloud sight lines has more than doubled the sample where H_3^+ is detected with measured H_2 (up to 21)
- Gaia extinction maps enable constraining the location of the absorbing gas along the line of sight
- Re-evaluation of gas densities determined from C_2 excitation reduces values by a factor of 4—7, having the same impact on inferred ionization rates

Future Prospects

- Expand H_3^+ survey in southern sky with VLT/CRIRES+
- Expand C_2 survey to provide more accurate densities in interstellar clouds
- Utilize other ionization rate tracers, e.g., OH^+
- Generate a map of cosmic-ray ionization rates in the local Milky Way